

Developing compact tuning fork thermometers for sub-mK temperatures and high magnetic fields

A.J. Woods, A.M. Donald, and L. Steinke

Department of Physics and National High Magnetic Field Laboratory High B/T Facility, University of Florida, Gainesville, FL 32611-8440, USA

(Dated: 1 April 2025)

The National High Magnetic Field Laboratory (NHMFL) High B/T facility at the University of Florida in Gainesville provides a unique combination of ultra-low temperatures below 1 mK and high magnetic fields up to 16 T for user experiments. To meet the growing user demand for calorimetric and thermal transport measurements, particularly on milligram-sized solid samples, we are developing scaleable thermometers based on quartz tuning fork resonators immersed in liquid ^3He . We demonstrate successful thermometer operation at the combined extreme conditions available at our user facility, and discuss the feasibility of fast and compact thermal probes.

I. INTRODUCTION

The NHMFL High B/T facility at the University of Florida in Gainesville pursues the mission to enable user experiments at the combined extremes of high magnetic fields and ultra-low temperatures (ULT) below 1 mK. While almost all measurement techniques like electrical transport or magnetometry require adaptations to be successfully performed in this environment, calorimetry and thermal transport are particularly challenging due to a lack of suitable thermometry. High-resolution thermal measurements in this regime would be of great benefit to the study of exotic Fermi surfaces via quantum oscillations, e. g. in the topological Kondo insulator SmB_6 ^{1,2} or other materials with charge-neutral fermi surfaces. Calorimetric measurements of quantum spin liquid (QSL) candidates could observe gapless excitations down to ultra-low temperatures, which would be important to demonstrate a QSL ground state³. Furthermore, thermal transport is a key experimental probe for the nodal structure of superconductors^{4,5}, and improved ULT thermometry could allow for studies of superconductors with extremely low transition temperatures such as bismuth⁶, as well as revealing characteristics of topologically non-trivial systems via the thermal Hall effect^{7,8}.

Motivated by these experimental challenges, we seek to develop thermometers that are suitable for measurements of typically milligram sized solid samples and are compatible with environments below 1 mK and high magnetic fields of 16 T and beyond. Existing thermometry options typically have at least one drawback that makes them unsuitable for these combined goals. Resistive thermometry has a minimum temperature of around 20 mK⁹, and SQUID noise thermometers^{10,11} are incompatible with high magnetic fields. ^3He melting curve thermometry¹² and nuclear magnetic resonance thermometers¹³ have too high masses and long thermalization times to allow for measurements of small samples. Coulomb blockade thermometers show promise as ultra-low temperature thermometers¹⁴⁻¹⁷, but typically require delicate on-lead magnetic demagnetisation stages or on-chip cooling,

which makes them incompatible or too complicated to use as sample thermometers in high magnetic fields.

Here we investigate quartz tuning fork thermometry in liquid ^3He , which could potentially meet all of these experimental requirements. The measurement principle relies on the temperature dependent viscosity of liquid ^3He that is probed by tracking the resonance of quartz tuning forks immersed in the liquid. As quartz tuning forks are widely used in studies of the ULT properties of the helium liquids¹⁸⁻²¹ with a minimum temperature of 100 μK in ^3He , their compatibility with a ULT environment is well established. In addition, thermometers tracking the vacuum resonance of a tuning fork have been used at intermediate magnetic fields up to 8 T²², and magnetometers based on tuning forks in ^4He exchange gas have even been successfully operated at high magnetic fields up to 64 T and at temperatures around 1.3 K^{23,24}. Here we report on first measurements that subject quartz tuning fork thermometers filled with liquid ^3He to the combined extremes of ultra-low temperatures down to 1 mK and high magnetic fields up to 14.5 T. Furthermore, since the tuning forks measure viscosity - an intrinsic property of the ^3He liquid - the thermometer signal does not depend on its mass, potentially allowing for miniaturized temperature probes for studies on small solid samples. We discuss recent progress in realizing such thermometers, and establish current resolution limits for thermal measurements based on prototype dimensions and the resolution obtained in the experiments presented here.

II. EXPERIMENTS

A. Measurement Principles

1. Mechanical properties of quartz tuning forks

Tuning forks are piezoelectric resonators whose motion is driven by an AC voltage $V = V_0 e^{i\omega t}$, which induces deflection of the tines via the piezoelectric effect. The

stress caused by this deflection induces a current, which is maximum when the frequency of the driving signal matches the resonant frequency of the tines. The force on the tuning fork tines is given by

$$F = \frac{aV}{2}, \quad (1)$$

where a is the tuning fork constant. The response current is:

$$I = av, \quad (2)$$

where v is the velocity of the tips of the tuning fork tines. The tuning fork constant a depends on the dimensions of the tuning fork and the material properties of the quartz, it is given by²⁵:

$$a = 3d_{11}E\frac{\mathcal{T}\mathcal{W}}{\mathcal{L}}, \quad (3)$$

where d_{11} is the longitudinal piezoelectric modulus of quartz, E is the Young's modulus and \mathcal{T}, \mathcal{W} and \mathcal{L} are the dimensions of the tuning fork tines (figure 2).

In practice, the tuning fork constant can be derived directly from the properties of the resonance of the tuning fork (see appendix), yielding

$$a = \sqrt{\frac{4\pi m_e I_0 \Delta f}{V_0}}, \quad (4)$$

where I_0 is the response current amplitude at resonance, Δf is the width of the tuning fork resonance and $m_e = 0.25\rho_q\mathcal{L}\mathcal{W}\mathcal{T}$ is the effective mass of a tuning fork tine. $\rho_q = 2659 \text{ kg m}^{-3}$ is the density of quartz.

The tuning fork resonance is characterised by sweeping the frequency of the driving signal through the resonance at constant driving amplitude. The in-phase component, X of the response is given by the real part of equation A.3, where

$$X = \frac{Af_0f\Delta f}{(f_0^2 - f^2)^2 + (f\Delta f)^2}, \quad (5)$$

and the out-of-phase component Y is the imaginary part

$$Y = \frac{Af_0\Delta f(f_0^2 - f^2)}{(f_0^2 - f^2)^2 + (f\Delta f)^2}, \quad (6)$$

Due to the measurement circuit, the tuning fork resonance will also have a non zero phase θ and a frequency dependent background, typically of the form $BG = a_0 + a_1f$. We then fit the equation:

$$v(f) = X \cos \theta + Y \sin \theta + (a_0 + a_1f) \quad (7)$$

to obtain the amplitude A , resonant frequency f_0 , resonance width Δf , phase θ and background coefficients a_0 and a_1 of the tuning fork resonance. The in-phase and out-of-phase components during a typical frequency sweep in vacuum are shown in figure 1.

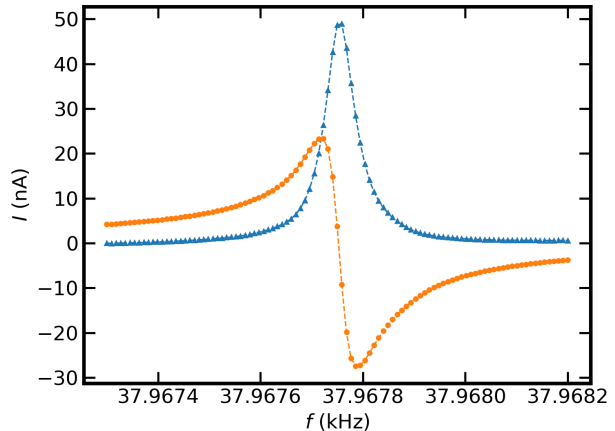


FIG. 1. A typical frequency sweep obtained in vacuum on the array tuning fork at $T = 1\text{K}$. The in-phase component is shown in blue and the out-of-phase in orange.

2. Tuning Forks in ^3He

The resonance width of the tuning fork Δf depends on the viscosity η of the ^3He as²⁵

$$\Delta f = \frac{1}{2} \sqrt{\frac{\rho\eta f_0}{\pi}} \mathcal{C} \mathcal{S} \frac{(f_0/f_{vac})^2}{m_{vac}}, \quad (8)$$

where \mathcal{C} is a geometric constant of order unity, which typically has a value around 0.6 for tuning forks of the type used here²⁶. $\mathcal{S} = 2\mathcal{L}(\mathcal{T} + \mathcal{W})$ is the surface area of the tuning fork tines and m_{vac} is the mass of a tuning fork tine. As the temperature dependence of the viscosity of ^3He is well known²⁷, the temperature can be calculated directly from the width of the tuning fork resonance. This calculation relies on \mathcal{C} and \mathcal{S} being known, the vacuum resonance properties of the tuning fork are well-known and characterised and that the force exerted by the surrounding fluid on the tuning fork tines is well-described by the Navier-Stokes equations. This last assumption holds true at temperatures above 0.6 mK and where the fluid viscosity is sufficiently small that the viscous penetration depth δ is smaller than the tuning fork tine spacing. The viscous penetration depth is

$$\delta = \sqrt{\frac{\eta}{\rho\pi f}}. \quad (9)$$

δ becomes similar to the dimensions of the tuning forks at the lowest temperatures studied here and therefore corrections may be needed in this regime.

B. Preparation of the tuning forks

In this work, we have investigated the ultra low temperature, high magnetic field properties of the two types

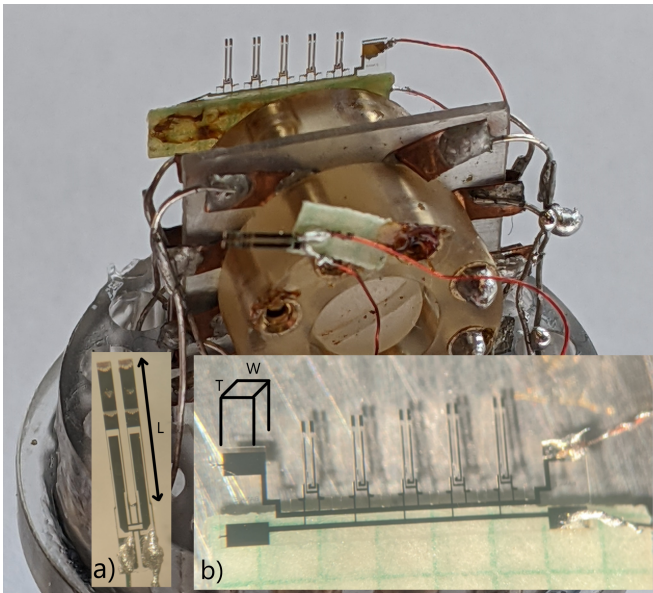


FIG. 2. The polycarbonate cell insert used in this work, showing the CTF (front) and Array of tuning forks (back). Inset: the tuning forks studied in this work. a) an Epson C-002RX commercial tuning fork (CTF), nominal resonance frequency 32.768 kHz. b) an array of 5 tuning forks, provided by Viktor Tsepelin, Lancaster University, UK²⁸.

of quartz tuning forks shown in the inset of figure 2 and whose physical dimensions are summarised in table I, the Epson C-002RX and an array of quartz tuning forks²⁸. The Epson tuning fork, hereafter referred to as the commercial tuning fork or CTF, is a readily commercially available device. The array of tuning forks was manufactured by Statek corporation for use in previous work on quantum turbulence in superfluid ^3He ²⁸.

The CTFs come in a vacuum tight can which must first be removed to expose it to the surrounding fluid. Removing the vacuum can is typically accomplished by carefully crushing the fibreglass base with pliers until the fork can be removed. Additionally, the leads that come soldered to the tuning fork are magnetic. For high field experiments, these leads must be removed and replaced. This is achieved by touching a fine soldering iron to the existing leads to remove them and replacing them with contacts made using Electron Microscopy Sciences 12642-14 silver epoxy. The silver epoxy contacts are then cured by baking on a hot plate at 70 °C for 15 mins to improve mechanical and chemical stability. Afterwards, the CTF was mounted to a piece of stycast 1266-impregnated graph paper, and the leads were glued to the paper with stycast to improve mechanical stability. The stycast paper was then attached to a polycarbonate insert for a ^3He cell shown in figure 2 and the leads soldered into the contact pins in the cell.

The array of tuning forks is patterned onto a quartz wafer of thickness 75 μm . It was carefully removed from tabs on the wafer by scoring with a scribing tool and

TABLE I. Summary of the dimensions of the tuning forks used in this work.

Tuning Fork	\mathcal{L} , μm	\mathcal{T} , μm	\mathcal{W} , μm	a , C m^{-1}	Δf_{vac} , Hz
CTF	3000	300	100	2.96×10^{-6}	0.110
ATF5	1450	90	75	8.42×10^{-7}	0.070

mounted on a piece of stycast paper. Contacts were made with EMS silver epoxy and the stycast paper mounted on the same cell insert as the CTF. During testing in room temperature air we established that the highest frequency tuning fork on this array showed the strongest resonant response, and therefore decided to focus on this tuning fork in the measurements presented here. This tuning fork is hereafter referred to as ATF5.

The cell insert was mounted in a ^3He cell in the experimental space of the Bay 3 cryostat at the NHMFL High B/T Facility. This cryostat is equipped with a PrNi₅/Cu nuclear demagnetisation stage precooled by a dilution refrigerator and a high field superconducting magnet capable of reaching temperatures of 1 mK and magnetic fields of 16 T simultaneously. The cell itself was attached to the end of a silver cold finger that provides thermal contact to the nuclear stage. The cell gets filled with liquid ^3He . The ^3He is cooled by a sintered silver heat exchanger which is bolted to the cold finger. The tuning forks are immersed in the liquid ^3He and so their resonant properties provide a direct measurement of the viscosity, and hence the temperature of the ^3He . The cryostat is also equipped with a ^3He melting curve thermometer, which is mounted in the zero field space above the nuclear stage and provides an independent measurement of the cell temperature, provided sufficient time for thermal relaxation of the system along the length of the silver cold finger between the nuclear stage and the ^3He cell is allowed.

The tuning fork resonance curves were characterised using the setup shown in figure 3. The AC driving voltage was supplied using a Keysight 33500B arbitrary waveform generator. Both sides of the tuning forks were connected to the inner conductor of coaxial leads, which were heat sunk at the various stages of the dilution refrigerator and finally at the nuclear stage. The outer conductors of the coaxial lines were connected together near the nuclear stage and grounded to the shared cryostat ground. The response current from the tuning fork was converted to a voltage using a home-built current to voltage converter (gain 10^4) and measured with a Stanford Research SR830 lock-in amplifier referenced to driving signal from the waveform generator.

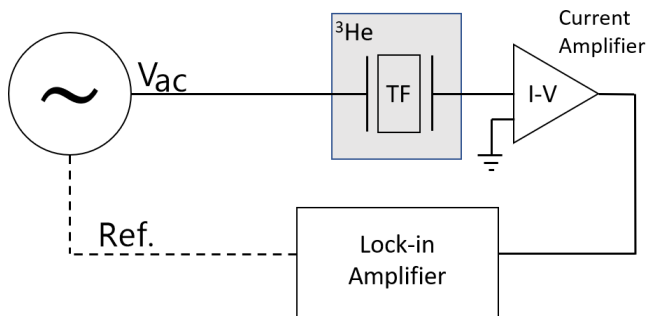


FIG. 3. Schematic of the measurement setup for the tuning fork resonance curves. Shaded in grey is the low temperature, high magnetic field region where the tuning forks are immersed in liquid ^3He .

TABLE II. A summary of the resonant widths of each tuning fork for different temperatures in normal fluid ^3He .

Temperature [mK]	CTF Δf [Hz]	ATF5 Δf [Hz]
100	40	90
30	120	300
10	410	950

C. Results

1. Vacuum Properties

Use of the tuning forks as thermometers requires knowledge of the vacuum resonance frequency and width. We therefore took care to measure the properties in vacuum at $T \leq 1.5\text{K}$. This temperature was chosen to minimise the residual vapour pressure in the cell, and obtain a resonance as close to the natural resonance as possible. The dimensions of the tuning forks and the vacuum properties are shown in table I.

2. Temperature Dependence

To measure temperature dependence, the tuning forks were constantly swept as the temperature was changed and the temperature was swept by magnetising and demagnetising the nuclear stage of the cryostat, providing access to the desired temperature range of 1mK - 100mK. It is assumed that the temperature change is sufficiently slow that the ^3He surrounding the tuning fork is thermalised more quickly than the time required to record a tuning fork resonance curve.

Figure 4 shows the measured resonance curves for ATF5 and CTF, for three different temperatures in the ^3He . The width of the resonance depends strongly on the viscosity of the ^3He , which increases significantly as the temperature decreases. (Summarised in table II). The resonance width of ATF5 is larger at all temperatures.

Figure 5 shows the width of ATF5 and CTF resonances

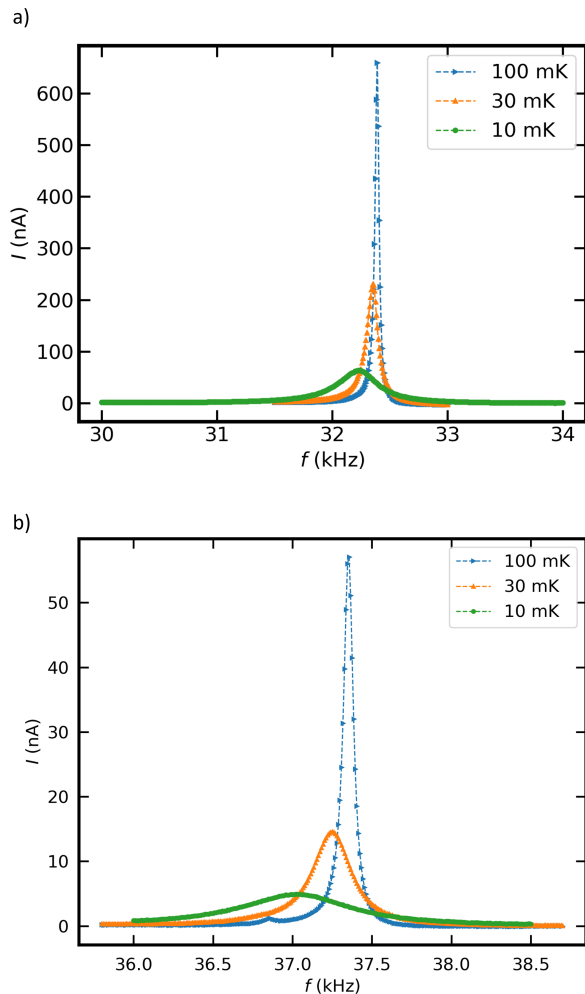


FIG. 4. Resonance curves (response current as a function of frequency) for a) CTF and b) ATF5 at 10, 30 and 100 mK in normal fluid ^3He .

as a function of temperature during the cooldown from 140 mK to 1 mK. ATF5 is more sensitive to the ^3He viscosity. It shows a stronger temperature dependence for $6\text{ mK} \leq T \leq 140\text{ mK}$, but becomes almost impossible to measure in the high viscosity regime below 6 mK. The CTF is measurable through most of the range of interest, presenting difficulties as the temperature approaches 1.5 mK, which is attributed to difficulties fitting the resonance curve when the tuning fork damping becomes so large that the measured signal is small compared to the background. The fitting is significantly improved by allowing the fitting procedure to use a background that is quadratic in frequency.

3. High Field Tests

To test the performance of the tuning forks in high magnetic fields, we took two approaches. The first, shown in

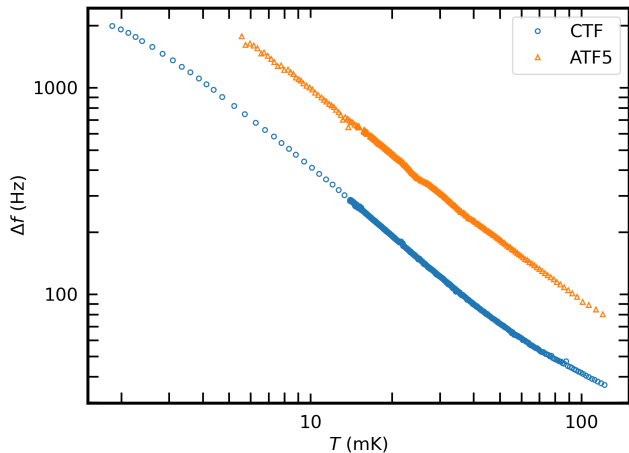


FIG. 5. The resonance width as a function of nuclear stage temperature for CTF (blue circles) and ATF5 (orange triangles).

figure 6 was to sweep the magnetic field at an approximately constant temperature near the base temperature of the dilution unit. Figure 6a) shows the width of ATF5 as a function of the applied magnetic field. The width changes as the field is changed, and relaxes while the field remains constant. We attribute this to eddy current heating in the silver cold finger that links the nuclear stage to the ^3He cell. The change in width is linked to a change in the temperature of the ^3He in the cell, which is shown in 6b), where the temperature is derived from the MCT at the top of the nuclear stage. Figure 6c) shows the tuning fork constant as a function of the applied field. While the tuning fork resonance shows a direct response to the temperature changes in the cell, the tuning fork constant remains within 0.6 % of its $B = 0$ value even at the highest field of 14.5 T. This confirms that there is no significant magnetic field induced effect on the properties of the quartz or the tuning fork electrodes, and that the tuning fork is suitable as a high magnetic field thermometer in the ULT regime.

The behaviour of the CTF in applied magnetic fields was investigated by measuring the resonance as the temperature was reduced during demagnetisations at zero applied magnetic field and at 14.5 T. The tuning fork constant as a function of temperature during these demagnetisations is shown in figure 7. It is clear here that the change in magnetic field does not have an effect on the tuning fork constant. The tuning fork constant does however begin to deviate to a lower value as the temperature approaches 1 mK, and this is attributed to the fact that the viscous penetration depth becomes comparable to the inter-tine spacing in this temperature regime and that fitting of the resonance curve becomes difficult.

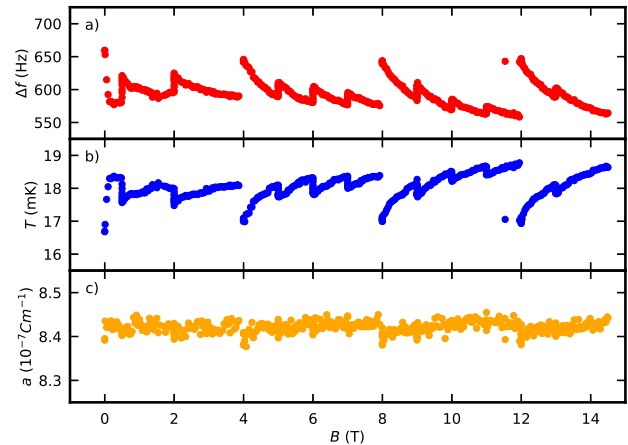


FIG. 6. a) The resonance width of ATF5 as function of applied magnetic field during a sequence of field sweeps. b) The temperature inferred from the melting curve thermometer during the same field sweeps. c) The tuning fork constant, as calculated from the fitted resonance curve as a function of the applied field.

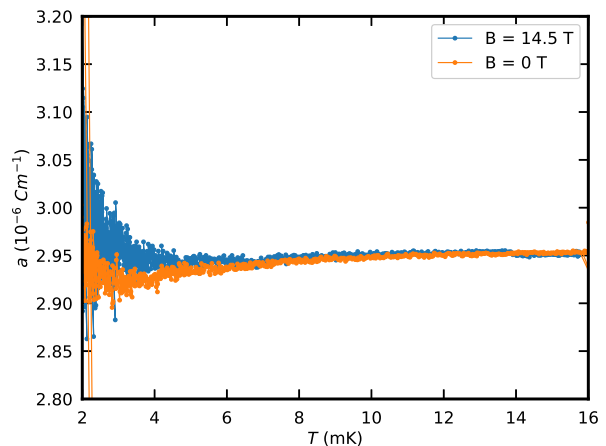


FIG. 7. The tuning fork constant of the CTF as a function of the cell temperature during two nuclear demagnetizations, at 0 T (orange circles) and 14.5 T (blue triangles).

D. Tuning forks in ^3He as thermal probes for small samples

To adapt the tuning fork thermometry to specific heat and thermal transport measurements of small samples, the thermal mass of the thermometer must be small enough that temperature changes caused by the thermal response of the sample can be detected. A lower thermal mass also corresponds to a faster response time of the thermometer, which allows for measurements with higher resolution. This can be achieved by reducing the ^3He volume as much as possible, since the dominant contribution to the ULT specific heat of ^3He cells generally

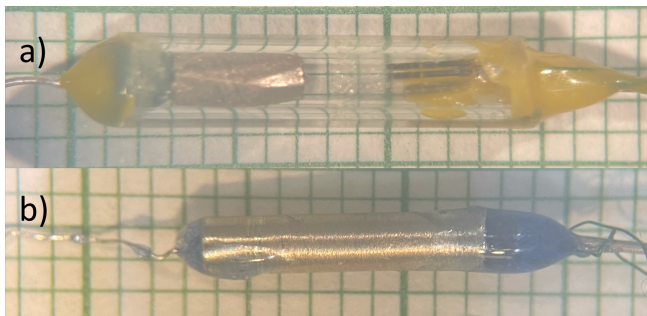


FIG. 8. Prototype tuning fork thermometers comprising a CTF and silver sinter heat exchanger encased in a) a quartz tube and b) a silver tube. The squares in the background are each 1 mm.

stems from the liquid itself. As the tuning fork directly probes the viscosity of the surrounding liquid, its measurement signal is independent of the total ^3He mass. Reducing the amount of ^3He should not come at the expense of temperature resolution or alter the measurement result, as long as the tuning fork is not within the viscous penetration depth of the walls of the thermometer.

Figure 8 shows prototype tuning fork thermometers that represent first attempts at minimising the ^3He volume while still allowing for enough space for the tuning fork to ring freely, to add or remove ^3He via a fill capillary, and ensuring good thermal contact via an integrated heat exchanger. Both prototypes contain nominally identical CTFs and silver heat exchangers and are sealed with epoxy plugs at either end. The thermometer in panel a) is constructed from a transparent quartz capillary and shows the placement of the tuning fork and heat exchanger inside the sealed volume that will be filled with ^3He . Panel b) shows the smallest liquid ^3He thermometer cell we have constructed to date, with the thermometer body entirely made of high-purity silver. We estimate its total specific heat to be around $4 \mu\text{J K}^{-1}$, based on published values for ^3He ²⁷ and silver²⁹. The thermalisation time of the thermometer depends on the specific heat and the thermal resistance determined by the surface area of the silver heat exchanger³⁰. For a heat exchanger of the size shown in figure 8a), assuming a 50 % packing fraction, we calculate that the response time of the thermometer is of order 50 s, which is a comparably rapid response in the context of ULT experiments. Based on the accuracy of the measurement of the tuning fork width, we assume that the detection limit of the tuning fork thermometer is around 1% of its own specific heat, i. e. it should be capable of measuring samples with specific heat 40 nJ K^{-1} , comparable to the specific heat of small single crystal samples that users of the High B/T facility may want to investigate.

III. SUMMARY

We have shown that quartz tuning forks immersed in liquid ^3He provide robust thermometry at the combined extremes of ultra-low temperatures down to 1 mK and high magnetic fields up to 14.5 T, presenting a viable alternative to the much slower and more difficult to implement ^3He melting curve or NMR thermometry that is presently being used. Near 1 mK, the high viscosity of the normal fluid ^3He still presents challenges. The most fundamental is the effect of the viscous penetration depth on the tuning fork properties, which could be alleviated by careful design of the tuning fork dimensions. The high viscosity also leads to profound damping of the tuning fork resonance, which becomes difficult to detect on top of a large measurement background. A careful characterisation of the background and optimisation of resonance fit routines could help to improve thermometer performance near this temperature. We further discussed the feasibility of miniature thermometers that could provide much needed thermal probes for user experiments on small solid state samples in the extreme environments accessible at the NHMFL High B/T Facility. Existing thermometer prototypes built with relatively simple fabrication methods could already be suitable for a large number of measurements extending the typical temperature range for thermal measurements below ~ 20 mK.

Appendix: Electromechanical model of the quartz tuning fork

To describe the properties of the tuning fork resonance in fluid we model each tine as a damped harmonic oscillator with effective mass m_e and spring constant k .

The equation of motion is

$$\frac{d^2u(t)}{dt^2} + \gamma \frac{du(t)}{dt} + \omega_0^2 u(t) = \frac{F(t)}{m_e}, \quad (\text{A.1})$$

where $u(t)$ is the displacement along the prong, γ describes the drag force, $F(t) = F_0 e^{i\omega t}$ is the driving force and $\omega_0 = k/m_e$ is the vacuum resonance frequency. Modelling each prong as an ideal cantilever, the effective mass of the prong is:

$$m_e = \rho_q \mathcal{L} \mathcal{W} T. \quad (\text{A.2})$$

In a fluid, γ has real and imaginary components, $\gamma = \gamma_2 + i\gamma_1$ where γ_2 describes dissipative drag forces while γ_1 describes the non-dissipative force arising from the fluid backflow.

Solving equation A.1 for the velocity $v = du/dt = v_0 e^{i\omega t}$ of the tip of the tuning fork tine gives a velocity amplitude

$$v_0 = \frac{F_0 \gamma_2 \omega^2 - i\omega(\omega_0^2 - \omega^2 - \omega\gamma_1)}{m_e (\omega_0^2 - \omega^2 - \omega\gamma_1)^2 + \gamma_2^2 \omega^2}. \quad (\text{A.3})$$

Assuming that γ_1 and γ_2 are constants much less than the resonant frequency, equation A.3 describes a Lorentzian lineshape with width $\Delta f = \gamma_2/2\pi$.

At resonance, the tip velocity is maximum and has a value:

$$v_r = \frac{F_0}{2\pi m_e \Delta f}. \quad (\text{A.4})$$

Using this along with equations 1 and 2 we can write the tuning fork constant:

$$a = \sqrt{\frac{4\pi m_e I_0 \Delta f}{V_0}}. \quad (\text{A.5})$$

ACKNOWLEDGMENTS

All experiments were performed at the National High Magnetic Field Laboratory (NHMFL) High B/T Facility at the University of Florida. The NHMFL is supported by the National Science Foundation Cooperative Agreement DMR-1644779 and the State of Florida. The authors also acknowledge support from the NHMFL User Collaboration Grants Program (UCGP) project no. R00002799. The quartz tuning fork array was provided by Viktor Tsepelin, Lancaster University, UK.

¹B. S. Tan, Y.-T. Hsu, B. Zeng, M. C. Hatnean, N. Harrison, Z. Zhu, M. Hartstein, M. Kiourlappou, A. Srivastava, M. D. Johannes, T. P. Murphy, J.-H. Park, L. Balicas, G. G. Lonzarich, G. Balakrishnan, and S. E. Sebastian, "Unconventional fermi surface in an insulating state," *Science* **349**, 287–290 (2015).

²M. Hartstein, W. H. Toews, Y.-T. Hsu, B. Zeng, X. Chen, M. C. Hatnean, Q. R. Zhang, S. Nakamura, A. S. Padgett, G. Rodway-Gant, J. Berk, M. K. Kingston, G. H. Zhang, M. K. Chan, S. Yamashita, T. Sakakibara, Y. Takano, J.-H. Park, L. Balicas, N. Harrison, N. Shitsevalova, G. Balakrishnan, G. G. Lonzarich, R. W. Hill, M. Sutherland, and S. E. Sebastian, "Fermi surface in the absence of a fermi liquid in the kondo insulator SmB₆," *Nature Physics* **14**, 166–172 (2017).

³C. Broholm, R. J. Cava, S. A. Kivelson, D. G. Nocera, M. R. Norman, and T. Senthil, "Quantum spin liquids," *Science* **367**, eaay0668 (2020).

⁴Y. Matsuda, K. Izawa, and I. Vekhter, "Nodal structure of unconventional superconductors probed by angle resolved thermal transport measurements," *Journal of Physics: Condensed Matter* **18**, R705–R752 (2006).

⁵M. Sutherland, J. Dunn, W. H. Toews, E. O'Farrell, J. Analytis, I. Fisher, and R. W. Hill, "Low-energy quasiparticles probed by heat transport in the iron-based superconductor LaFePO," *Physical Review B* **85**, 014517 (2012).

⁶O. Prakash, A. Kumar, A. Thamizhavel, and S. Ramakrishnan, "Evidence for bulk superconductivity in pure bismuth single crystals at ambient pressure," *Science* **355**, 52–55 (2016).

⁷M. Kawano and C. Hotta, "Thermal hall effect and topological edge states in a square-lattice antiferromagnet," *Physical Review B* **99**, 054422 (2019).

⁸X.-T. Zhang, Y. H. Gao, C. Liu, and G. Chen, "Topological thermal hall effect of magnetic monopoles in the pyrochlore u(1) spin liquid," *Physical Review Research* **2**, 013066 (2020).

⁹S. S. Courts, J. K. Krause, J. G. Weisend, J. Barclay, S. Breon, J. Demko, M. DiPirro, J. P. Kelley, P. Kittel, A. Klebaner, A. Zeller, M. Zagarola, S. V. Sciver, A. Rowe, J. Pfothenhauer, T. Peterson, and J. Lock, "A COMMERCIAL RUTHENIUM OXIDE THERMOMETER FOR USE TO 20 MILLIKELVIN," in *AIP Conference Proceedings* (AIP, 2008).

¹⁰D. Rothfuss, A. Reiser, A. Fleischmann, and C. Enss, "Noise thermometry at ultra-low temperatures," *Philosophical Transactions of the Royal Society A: Mathematical, Physical and Engineering Sciences* **374**, 20150051 (2016).

¹¹A. Kirste and J. Engert, "A SQUID-based primary noise thermometer for low-temperature metrology," *Philosophical Transactions of the Royal Society A: Mathematical, Physical and Engineering Sciences* **374**, 20150050 (2016).

¹²W. Ni, J. S. Xia, E. D. Adams, P. S. Haskins, and J. E. McKisson, "3He melting pressure temperature scale below 25 mK," *Journal of Low Temperature Physics* **99**, 167–182 (1995).

¹³R. Tycko, "NMR at low and ultralow temperatures," *Accounts of Chemical Research* **46**, 1923–1932 (2013).

¹⁴J. P. Pekola, J. J. Toppari, J. P. Kauppinen, K. M. Kinnunen, A. J. Manninen, and A. G. M. Jansen, "Coulomb blockade-based nanothermometry in strong magnetic fields," *Journal of Applied Physics* **83**, 5582–5584 (1998).

¹⁵L. Casparis, M. Meschke, D. Maradan, A. C. Clark, C. P. Scheller, K. K. Schwarzwalder, J. P. Pekola, and D. M. Zumbühl, "Metallic coulomb blockade thermometry down to 10 mK and below," *Review of Scientific Instruments* **83**, 083903 (2012).

¹⁶M. Palma, C. P. Scheller, D. Maradan, A. V. Feshchenko, M. Meschke, and D. M. Zumbühl, "On-and-off chip cooling of a coulomb blockade thermometer down to 2.8 mK," *Applied Physics Letters* **111**, 253105 (2017).

¹⁷N. Yurttagül, M. Sarsby, and A. Geresdi, "Coulomb blockade thermometry beyond the universal regime," *Journal of Low Temperature Physics* (2021), 10.1007/s10909-021-02603-w.

¹⁸D. I. Bradley, M. Človečko, S. N. Fisher, D. Garg, E. Guise, R. P. Haley, O. Kolosov, G. R. Pickett, V. Tsepelin, D. Schmoranzner, and L. Skrbek, "Crossover from hydrodynamic to acoustic drag on quartz tuning forks in normal and superfluid ⁴He," *Physical Review B* **85**, 014501 (2012).

¹⁹S. L. Ahlstrom, D. I. Bradley, M. Človečko, S. N. Fisher, A. M. Guénault, E. A. Guise, R. P. Haley, O. Kolosov, P. V. E. McClintock, G. R. Pickett, M. Poole, V. Tsepelin, and A. J. Woods,

- “Frequency-dependent drag from quantum turbulence produced by quartz tuning forks in superfluid ^4He ,” *Physical Review B* **89**, 014515 (2014).
- ²⁰M. J. Jackson, O. Kolosov, D. Schmoranzer, L. Skrbek, V. Tsepelin, and A. J. Woods, “Measurements of vortex line density generated by a quartz tuning fork in superfluid ^4He ,” *Journal of Low Temperature Physics* **183**, 208–214 (2015).
- ²¹D. O. Clubb, O. V. L. Buu, R. M. Bowley, R. Nyman, and J. R. Owers-Bradley, “Quartz tuning fork viscometers for helium liquids,” *Journal of Low Temperature Physics* **136**, 1–13 (2004).
- ²²M. Človečko and P. Skyba, “Quartz tuning fork—a potential low temperature thermometer in high magnetic fields,” *Applied Physics Letters* **115**, 193507 (2019).
- ²³K. A. Modic, M. D. Bachmann, B. J. Ramshaw, F. Arnold, K. R. Shirer, A. Estry, J. B. Betts, N. J. Ghimire, E. D. Bauer, M. Schmidt, M. Baenitz, E. Svanidze, R. D. McDonald, A. Shekhter, and P. J. W. Moll, “Resonant torsion magnetometry in anisotropic quantum materials,” *Nature Communications* **9** (2018), 10.1038/s41467-018-06412-w.
- ²⁴K. A. Modic, R. D. McDonald, J. P. C. Ruff, M. D. Bachmann, Y. Lai, J. C. Palmstrom, D. Graf, M. K. Chan, F. F. Balakirev, J. B. Betts, G. S. Boebinger, M. Schmidt, M. J. Lawler, D. A. Sokolov, P. J. W. Moll, B. J. Ramshaw, and A. Shekhter, “Scale-invariant magnetic anisotropy in RuCl_3 at high magnetic fields,” *Nature Physics* **17**, 240–244 (2020).
- ²⁵R. Blaauwgeers, M. Blazkova, M. Človečko, V. B. Eltsov, R. de Graaf, J. Hosio, M. Krusius, D. Schmoranzer, W. Schoepe, L. Skrbek, P. Skyba, R. E. Solntsev, and D. E. Zmeev, “Quartz tuning fork: Thermometer, pressure- and viscometer for helium liquids,” *Journal of Low Temperature Physics* **146**, 537–562 (2007).
- ²⁶D. I. Bradley, M. Človečko, S. N. Fisher, D. Garg, A. M. Guénault, E. Guise, R. P. Haley, G. R. Pickett, M. Poole, and V. Tsepelin, “Thermometry in normal liquid ^3He using a quartz tuning fork viscometer,” *Journal of Low Temperature Physics* **171**, 750–756 (2012).
- ²⁷D. S. Greywall, “ ^3He specific heat and thermometry at millikelvin temperatures,” *Physical Review B* **33**, 7520–7538 (1986).
- ²⁸S. L. Ahlstrom, D. I. Bradley, S. N. Fisher, A. M. Guénault, E. A. Guise, R. P. Haley, S. Holt, O. Kolosov, P. V. E. McClintock, G. R. Pickett, M. Poole, R. Schanen, V. Tsepelin, and A. J. Woods, “A quasiparticle detector for imaging quantum turbulence in superfluid $^3\text{He-B}$,” *Journal of Low Temperature Physics* **175**, 725–738 (2014).
- ²⁹D. L. Martin, “Specific heat of copper, silver, and gold below 30°K ,” *Physical Review B* **8**, 5357–5360 (1973).
- ³⁰J. Pollanen, H. Choi, J. P. Davis, B. T. Rolfs, and W. P. Halperin, “Low temperature thermal resistance for a new design of silver sinter heat exchanger,” *Journal of Physics: Conference Series* **150**, 012037 (2009).